Spontaneous Wave Pattern Formation in Vibrated Granular Materials

Keiko M. Aoki and Tetsuo Akiyama

Department of Chemical Engineering and Materials Science, Shizuoka University, 3-5-1 Johoku, Hamamatsu 432, Japan

(Received 12 March 1996; revised manuscript received 12 September 1996)

This paper presents two-dimensional particle dynamics simulations of a vertically vibrated layer of granules, wherein a spontaneous formation of parametric surface waves appears. The investigation of the dynamic process and mechanism that leads to the formation of the granular surface waves has revealed that the dissipation coefficient in shear direction plays a crucial role in the formation of wave patterns. Scaling relations between the units in simulations and experiments are evaluated. Simulation results are shown to compare well with experimental ones. [S0031-9007(96)01646-8]

PACS numbers: 46.10.+z, 02.70.Ns, 47.54.+r, 62.30.+d

Spatial patterns that can be observed in nature and in laboratories of diverse fields of science often exhibit strikingly similar features irrespective of their microscopic mechanisms. For instance, stripes appear in electrohydrodynamic convection of liquid crystals, in monomolecular organic films, and in chemical reaction-diffusion systems [1]. Hexagonal patterns can be found in crystals, in flat mounds of rocks on the bed of shallow lakes, in vibrated granulars, and even in fish territories [2,3].

Granular materials, when subjected to vertical vibrations, exhibit interesting patterns such as convection rolls [4] and waves [5,6]. Recently, it has been reported that multipairs of convection rolls [7], analogous to the Rayleigh-Bérnard convection in fluids, appear in the vibrated bed. Spatial patterns can be found not only in such stationary systems (in the sense that the pattern itself does not make time dependent cyclic changes) but also in oscillating systems. Melo, Umbanhowar, and Swinney [6] have reported parametric wave patterns in a vertically oscillated granular layer. The granular wave patterns have been reported to be similar to parametric surface wave patterns in fluid layers [8].

The basic macroscopic phenomenology of pattern formation has been successfully described by continuum models based on partial differential equations [1]. However, deeper understanding of the collective behavior calls for the investigation of microscopic mechanisms, for which the discrete multibody approach is most suited. Simulation studies (based on discrete models) on spatially stationary systems, such as convection rolls of granules under vibrations, have been done by many authors [9]. In the present study we focus attention on a oscillating system, and report a simulation study on two-dimensional (2D) particle dynamics of a vertically vibrated layer of granules. The present study shows that the spontaneous formation of surface waves, corresponding to those observed experimentally in a three-dimensional (3D) setup [6], can also be observed in 2D simulations. The simulations use reduced units, and the scaling relations between the units in simulations and in experiments are evaluated by comparing simulation results with experimental ones. We investigate the dynamic process of the pattern formation in granular layers and explain the underlying mechanism that leads to the pattern formation.

On pursuing particle dynamics, we postulate that the collective motion of granular materials can be described by the excluded volume effect and the dissipation of kinetic energy between granules. A simulation model based on the above postulates is described below [10]. We define a short-range repulsive force interacting between two particles,

$$\mathbf{f}_{ij} = -\frac{\partial \phi_{ij}}{\partial \mathbf{r}_{ij}}, \tag{1}$$

where ϕ_{ij} is

$$\phi_{ij} = \begin{cases} \varepsilon\left[\left(\frac{d}{\mathbf{r}_{ij}}\right)^{12} - \left(\frac{d}{\mathbf{r}_{ij}}\right)^{6} + \frac{1}{4}\right], & \text{if } |\mathbf{r}_{ij}| < r_0, \\ 0, & \text{otherwise.} \end{cases} \tag{2}$$

This pairwise interaction depends on the distance $\mathbf{r}_{ij}$ between the center of particles i and j within the range of $r_0 = 2^{1/6}d$, d being the characteristic length representing the particle size. In addition, we introduce the normal dissipation force

$$\mathbf{f}_i^{\text{normal}} = -\gamma_n m(\mathbf{v}_{ij} \cdot \mathbf{r}_{ij})\mathbf{r}_{ij}/|\mathbf{r}_{ij}|^2, \tag{3}$$

and the shear dissipation force

$$\mathbf{f}_i^{\text{shear}} = -\gamma_s m(\mathbf{v}_{ij} \cdot \mathbf{t}_{ij})\mathbf{t}_{ij}/|\mathbf{r}_{ij}|^2, \tag{4}$$

where γ_n and γ_s are, respectively, the normal and shear dissipation coefficients. The dissipation forces act at each contact point. Here, $\mathbf{v}_{ij}$ is the relative velocity, $\mathbf{t}_{ij} = (-r_{ij}^y, r_{ij}^x)$, and m is the mass of a particle. The same repulsive force is used to describe the interaction between the particles and the container (both the bottom and the walls), with $|\mathbf{r}_{ij}|$ being replaced by the distance between the container and particles. The container is subjected to continual sinusoidal vertical vibrations. Energy, length, and mass are scaled in units of ε, d, and m, respectively, then the intrinsic unit of time and acceleration become $(md^2/\varepsilon)^{1/2}$ and $\varepsilon/(md)$, respectively [11]. With the use of the intrinsic reduced units, the dissipation coefficients, γ_n and γ_s, remain as the only intrinsic free parameters.

 0031-9007/96/77(20)/4166(4)$10.00

Note that it is tacitly assumed, by scaling the length with d, that the effect of particle size can be accounted for by the difference in the values of dissipation coefficients. The validity of this assumption will be examined later. Here, we introduce a new unit of time $t_s = f_0 t^*$, where f_0 is the frequency number (hence dimensionless) of the externally applied vibration and t^* is the intrinsic reduced unit of time. The merit of using this time unit is that the time step dt can be made as a fixed fraction (1/2500 for simulations reported in this study) of a vibrational cycle. More importantly, it leads to a new reduced unit of gravitational acceleration, g_s, expressed below.

$$g_s = g\left(\frac{t}{t_s}\right)^2 \frac{1}{d} = \frac{g^*}{f_0^2}, \tag{5}$$

where g is the gravitational acceleration, and g^* is the intrinsic reduced gravitational acceleration. The value of g_s expresses the intrinsic effective gravitational acceleration in accord with the movement of the container. The introduction of g_s is significant in that it makes the simulation study on the frequency dependence of the granular bed possible without specifying the values of the intrinsic gravitational acceleration and the vibrational frequency. The value of intrinsic gravitational acceleration for a given system can be determined by comparing the simulation results with experimental ones. Simulations have been performed for systems of particle number $N = 735$, 1470, and 1960 in containers of width $W = 50$, 100, 150, and 200, with varying dissipation coefficients.

The dynamic process of pattern formation is revealed in Fig. 1 by the snapshots at different phases for the case of $N = 1470$, $W = 150$, $g_s = (2\pi)^2$, $A = 1.2$, and $\gamma_n = \gamma_s = 2$. Figure 1 shows that two vibration cycles of the container is necessary for one cycle of the pattern of the bed, furthermore, the wave number is not quantized by the boundary conditions (container width), five and a half heaps are formed in the container. The initial configuration of the granular bed affects the position where the heaps form but not the value of λ when $W \geq 100$, indicating that λ is determined intrinsically given the frequency with g_s fixed [12]. The above observations closely coincide with experimental ones by Melo *et al.* [6].

The dynamic process of the formation of parametric surface waves observed in simulations is explained below. When vertical vibration is applied to granular beds, density fluctuation occurs not only in the vertical direction but also in the lateral direction. The fluctuation first occurs near the walls and in the middle of the bed, then spreads throughout the bed. The density fluctuation in lateral direction leads to heap formation. Heaps form after the bed collides with the container of downward motion ($\pi/2$–$3\pi/2$, $5\pi/2$–$7\pi/2$ in Fig. 1). The particles are more densely packed at the positions where heaps form, and an air gap is seen at the bottom of the layer prior to the formation of heaps. Note also that some voids (1–2 particle size) exist near the bottom of the bed (π and 3π). These small voids grow, resulting in a bridge (or bridges) when the container width is sufficiently small. Such cases have been reported in experimental studies by Douady, Fauve, and Laroche [5]. When the container velocity is at a maximum ($2n\pi$ in Fig. 1), the bed gets highly compressed, which results in consolidating the wave structure. After the velocity passes through the maxima, the bed begins to dilate and the particles naturally fall from the heaps to the valleys. This particle flow continues, due to its lateral momentum, even after the bed surface is leveled, alternating the positions of heaps and valleys. This is why the surface wave pattern takes two vibrational cycles of the container to return to it's original state. The lateral movement of the particles is forced to halt when the bed collides with the bottom of the bed in the upward phase. The time span, when the container is in the upward phase, decreases with increasing frequency (decreasing g_s), thereby the distance particles can move in the lateral direction decreases. This explains why λ becomes small with frequency. Since g_s is the effective force that pulls down the particles in the valley, it is conceivable that λ becomes proportional to g_s, which, in fact, as will be shown later, turns out to be true in a certain range of g_s.

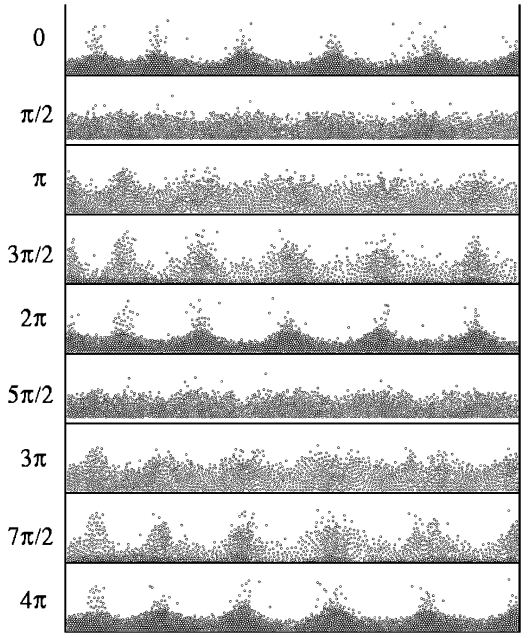

FIG. 1 Snapshots of a bed after 50 vibration cycles at phases 0, $\frac{\pi}{2}$, π, $\frac{3\pi}{2}$, 2π, $\frac{5\pi}{2}$, 3π, $\frac{7\pi}{2}$, and 4π. The number of particles $N = 1470$ and container width $W = 150$ for $\gamma_n = \gamma_s = 2$, $A = 1.2$, and $g_s = (2\pi)^2$. The particles are shown in effective core diameter, which is $d_{\text{eff}} = 0.71$ in the present dynamic state.

The shear dissipation force plays a crucial role in the pattern formation [13]. Simulation studies under two sets of conditions, $\gamma_n = \gamma_s = 1$ and $\gamma_n = 4$, $\gamma_s = 0$ did not lead to surface wave pattern formation, for reasons that the magnitudes of γ_n and γ_s were too small in the first case, and, in the second, there was no shear dissipation force even when γ_n was sufficiently large. The importance of γ_s

on the formation of surface wave patterns may be readily understood when one thinks of the fact that the angle of repose is strongly dependent on the magnitude of γ_s when the system is under perturbation. We may add that, even when the normal dissipation coefficient is much smaller ($\gamma_n = 0.4$, $\gamma_s = 0$), the density fluctuation occurred in the lateral direction, and heaps appeared momentarily, but they did not last long. This indicates that γ_s is not an important factor for the cause of the density fluctuation, but it plays a crucial role in maintaining the wave pattern.

We show in Fig. 2 the λ vs g_s relationship near the threshold vibration acceleration for the case of $N = 1960$ and $W = 200$ with varying dissipation coefficients. (I) $\gamma_s = \gamma_n = 2.0$ (symbol ∘), (II) $\gamma_s = \gamma_n = 4.0$ (symbol •), and (III) $\gamma_s = \gamma_n = 6.0$ (symbol □) [14]. The wavelength is measured after 100 vibration cycles. For convenience, we express g_s in the unit of $(2\pi)^2$. It can be seen from Fig. 2 that λ is linearly dependent on g_s for cases II and III, but for case I, the linear dependence saturates at a large g_s (or a low frequency): Wave patterns were not stable at $g_s = 2.25(2\pi)^2$. The g_s dependence of λ is summarized in the following relationship:

$$\lambda_s = \lambda_{s0} + \alpha g_s , \tag{6}$$

where λ_{s0} and α are to be determined from the least mean square fit for each system. Excluding the two data points for case I, we have $\lambda_{s0} = 9.1$ and $\alpha = 16.3/(2\pi)^2$ (if the last two data points are included, they become $\lambda_{s0} = 13.5$ and $\alpha = 12.2/(2\pi)^2$, respectively). For case II, we have $\lambda_{s0} = 8.7$, $\alpha = 18.1/(2\pi)^2$, and, for case III, $\lambda_{s0} = 7.0$, $\alpha = 21.4/(2\pi)^2$. Note that the wavelengths λ_s and λ_{s0} are measured in the unit of d. It has been reported in experimental studies that the wavelength λ for parametric patterns is linearly dependent on $1/f^2$, and the following relationship holds [6]:

$$\lambda = \lambda_0 + g_{\text{eff}}/f^2, \tag{7}$$

where $\lambda_0 \approx 11D$ and $g_{\text{eff}} \approx 310$ cm/s^2. Scaling Eq. (7) by the particle diameter D results in

$$\lambda/D = 11 + g_{\text{eff}}/Df^2. \tag{8}$$

Since $g_s \propto 1/f_0^2$, it can be readily seen that the above two equations (6) and (8) are basically the same in formula. The first terms on the right hand sides of Eqs. (6) and (8) represent the cutoff wavelengths, giving $\lambda_{s0} \simeq \lambda_0/D$ [15]. Equating the second terms on the right hand sides of Eqs. (6) and (8) yields

$$g^* = g_s f_0^2 = \frac{g_{\text{eff}}}{\alpha D}\left(\frac{f_0}{f}\right)^2, \tag{9}$$

where f_0/f is the unity in the unit of second. The gravitational acceleration is a universal constant, thus Eq. (9) leads to $\alpha D = \text{const}$. This implies, as α varies with dissipation coefficients, that the effect of granular size can be accounted for by the difference in the values of the dissipation coefficients, that is, the ratio $D_{\text{II}}/D_{\text{III}}$ can be replaced by $\alpha_{\text{III}}/\alpha_{\text{II}}$. This is the first time, as far as we know, that the relationship between the effect of particle size and that of dissipation coefficients on granular bed behavior is shown in an explicit form.

Comparison of our simulation results to experimental ones is significant in that it gives us quantitative scaling relationships between real values in experiments and simulation parameters. Of the parameters dealt with in this study the most important one is the gravitational acceleration. Here, a caution is needed; because our simulation is 2D, thus it is not clear whether the parametric waves in simulation correspond to the stripe or the square patterns in 3D experiments. Melo *et al.* report the frequency dependence of the pattern wavelength λ only for the case of square patterns in their experiments [6]. Thus, assuming that the simulated surface wave patterns correspond to the square patterns, we evaluate the parameter values. The experiment indicates that parametric square patterns only appear when $f < 28$ Hz [6], while, in the simulation, the wave patterns only appear for $g_s > 0.75(2\pi)^2$. Thus, substituting $f_0 = 28$ and $g_s = 0.75(2\pi)^2$ into Eq. (5), we have $g^* \simeq 590(2\pi)^2$. Equation (9) then yields $D = 0.32$ (0.43) mm for case I: The number in the parentheses indicates the value when the last two data points are included in the correlation. For cases II and III, we have $D = 0.29$ and 0.25 mm, respectively, which fall into the range surprisingly close to that of the experiments, 0.4, 0.3, and 0.2 mm. By using the above values of D and g^*, we obtain the λ vs $1/f^2$ relationship in units of mm and s^2 (inset in Fig. 2).

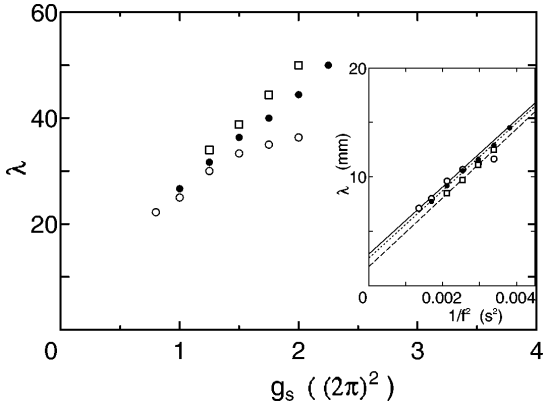

FIG. 2. Wavelength λ of the pattern vs g_s after 100 vibration cycles for $N = 1960$ and $W = 200$. (I) $\gamma_n = \gamma_s = 2.0$ (symbol ∘), (II) $\gamma_n = \gamma_s = 4.0$ (symbol •), and (III) $\gamma_n = \gamma_s = 6.0$ (symbol □). The inset shows the relationship λ (mm) vs $1/f^2$ (s^2).

It is shown in Fig. 3 that we can reproduce our results with a standard model [16] which uses interaction

$$V_{ij} = \begin{cases} k(d - |\mathbf{r}_{ij}|)^{5/2}, & \text{if } |\mathbf{r}_{ij}| < d , \\ 0, & \text{otherwise,} \end{cases} \tag{10}$$

with Eqs. (3) and (4). It should be mentioned, however, that, unlike the case of Eq. (2), Eq. (10) does not allow the scaling of r_{ij} (by d) independent of k. Consequently,

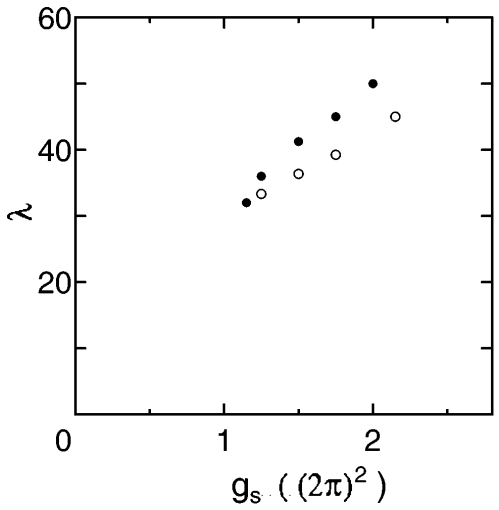

FIG. 3. Wavelength λ of the pattern vs g_s after 100 vibration cycles for $N = 1960$ and $W = 200$ with the standard model [Eq. (10)]: $k = 1.82 \times 10^4$ which corresponds to $\partial^2\phi_{ij}/\partial r_{ij}^2$ at $d_{\text{eff}} = 0.71$. (I) $\gamma_n = \gamma_s = 5.0$ (symbol ∘), and (II) $\gamma_n = \gamma_s = 10.0$ (symbol •).

the physical significance of Eqs. (5) and (9) lessens when used with Eq. (10).

In a recent experimental study, it is reported that the wave patterns become better defined when the air pressure in the container is reduced [3]. The square patterns are reported to appear only when $f < 40$ Hz for $D = 0.15$–0.19 mm bronze spheres. Substituting $f_0 = 40$ and $g_s = 0.75(2\pi)^2$ into Eq. (5), we have $g_s = 1200(2\pi)^2$, which, combined with Eq. (9), gives $D = 0.16$ (0.21), 0.14, and 0.12 mm for cases I, II, and III, respectively, again showing a good agreement with the experimental values.

In the two studies mentioned above, experiments are carried out under different conditions using different materials: glass beads in surrounding air [6] and bronze spheres under reduced air pressure [3]. They report that the differences in stiffness (restitution coefficients) and ambient air have no qualitative influence on the wave patterns [3]. The good quantitative agreement between the experimental and simulation results suggests that the excluded volume effect, combined with the dissipation of kinetic energy between granules, can describe the surface wave patterns well. To assess if this holds for a wider range of systems, additional experimental data are needed.

We have conducted computer simulations of particle dynamics, specifically on the parametric surface waves in vertically vibrated granular layers. It has been revealed that the dissipation coefficients play a significant role in the formation of surface wave patterns. The dynamic process leading to the pattern formation has been analyzed in detail. A comparison of simulation results with experimental ones enables us to determine the intrinsic reduced units of given systems. A good agreement between simulations and experiments proves that the basic features of granular materials can be described by the excluded volume effect and the dissipation of kinetic energy between granules.

[1] For a review, see M. C. Cross and P. C. Hohenberg, Rev. Mod. Phys. **65**, 851 (1993).

[2] I. Stewart and M. Golubitsky, *Fearful Symmetry* (Blackwell, Oxford, 1992).

[3] F. Melo, P. Umbanhowar, and H. L. Swinney, Phys. Rev. Lett. **75**, 3838 (1995).

[4] C. Laroche, S. Douady, and S. Fauve, J. Phys. (France) **50**, 699 (1989); P. Evesque and J. Rajchenbach, Phys. Rev. Lett. **62**, 44 (1989); J. Rajchenbach, Europhys. Lett. **16**, 149 (1991); E. Clement, J. Duran, and J. Rajchenbach, Phys. Rev. Lett. **69**, 1189 (1992); H. K. Pak, E. Van Doorn, and R. P. Behringer, Phys. Rev. Lett. **74**, 4643 (1995).

[5] S. Douady, S. Fauve, and C. Laroche, Europhys. Lett. **8**, 621 (1989).

[6] F. Melo, P. Umbanhowar, and H. L. Swinney, Phys. Rev. Lett. **72**, 172 (1994).

[7] K. M. Aoki, T. Akiyama, Y. Maki, and T. Watanabe, Phys. Rev. E **54**, 874 (1996).

[8] S. Fauve, K. Kumar, C. Laroche, D. Beysens, and Y. Garrabos, Phys. Rev. Lett. **68**, 3160 (1992); J. Bechhoefer, V. Ego, S. Manneville, and B. Johnson, J. Fluid Mech. **288**, 325 (1995).

[9] Y-h. Taguchi, Phys. Rev. Lett. **69**, 1367 (1992); J. A. C. Gallas, H. J. Herrmann, and S. Sokolowski, Phys. Rev. Lett. **69**, 1371 (1992); J. Lee, J. Phys. A **27**, L257 (1994); S. Luding, E. Clément, A. Blumen, J. Rajchenbach, and J. Duran, Phys. Rev. E **50**, R1762 (1994).

[10] K. M. Aoki and T. Akiyama, Phys. Rev. E **52**, 3288 (1995). When constructing the model, we had in mind the scaling relationship for soft-core models (inverse power potentials $\phi_{ij} = \varepsilon(r_{ij}/d)^{-n}$, including hard-core models as a case, $n = \infty$) in which the state of the system is uniquely defined by the reduced density $\rho^* = Nd_{\text{eff}}^2/V$. The effective core diameter d_{eff} is determined from the relationship $\phi(d_{\text{eff}}) = E_k$, where E_k is the average kinetic energy per particle.

[11] M. P. Allen and D. J. Tidesley, *Computer Simulations of Liquids* (Oxford University Press, Oxford, 1987).

[12] There is a tendency that λ becomes small when the layer thickness is small (for instance, in the system of $N = 735$ and $W = 200$). We may add that periodic boundary conditions quantize the wave number.

[13] The importance of the shear dissipation coefficient for other granular phenomena has been pointed out by P. K. Haff and B. T. Werner [Powder Technol. **48**, 239 (1986)] for segregation and Gallas *et al.* [9] for convection.

[14] An order of magnitude analysis indicates that the values of γ_s and γ_n used in this study give rise to shear stress of the order of 10^1 Pa at the wall, which is in good agreement with experimental measurements. [T. Akiyama and T. Shimomura, Powder Technol. **66**, 243 (1991).

[15] Considering that d_{eff} is approximately 30% smaller than d (the unit of length), the cutoff wavelength λ_{s0} in simulations becomes 10–13 in the unit of d_{eff}.

[16] O. R. Walton, Mech. Mater. **16**, 239 (1993); R. S. Sinkovits and S. Sen, Phys. Rev. Lett. **74**, 2686 (1995); J. Schäfer, S. Dippel, and D. E. Wolf, J. Phys. (Paris) **6**, 5 (1996).